Atmos. Chem. Phys. Discuss., 13, 22337–22381, 2013
www.atmos-chem-phys-discuss.net/13/22337/2013/
doi:10.5194/acpd-13-22337-2013

Atmospheric Chemistry and Physics Discussions

Aerosols and nucleation in Eastern China: first insights from the new SORPES-Station

E. Herrmann[1,2,*], A. J. Ding[1], V.-M. Kerminen[2], T. Petäjä[2], X. Q. Yang[1], J. N. Sun[1], X. M. Qi[1], H. Manninen[2], J. Hakala[2], T. Nieminen[2], P. P. Aalto[2], M. Kulmala[2], and C. B. Fu[1]

[1]School of Atmospheric Sciences & Institute for Climate and Global Change Research, Nanjing University, Nanjing, China
[2]Department of Physics, University of Helsinki, Helsinki, Finland
[*]now at: Paul Scherrer Institut, Villigen, Switzerland

Received: 5 July 2013 – Accepted: 22 August 2013 – Published: 28 August 2013

Correspondence to: E. Herrmann (erik.herrmann@iki.fi) and A. J. Ding (dingaj@nju.edu.cn)

Published by Copernicus Publications on behalf of the European Geosciences Union.

Abstract

Aerosols and new particle formation were studied in the western part of the Yangtze River Delta (YRD), at the SORPES station of Nanjing University. Air ions in the diameter range 0.8–42 nm were measured using an air ion spectrometer, and a DMPS provided particle number size distributions between 6 and 800 nm. Additionally, meteorological data, trace gas concentrations, and $PM_{2.5}$ values were recorded. During the measurement period from 18 November 2011 to 31 March 2012, the mean total particle concentration was found to be 23 000 cm^{-3}. The mean $PM_{2.5}$ value was 90 $\mu g\,m^{-3}$, well above national limits. During the observations, 26 new particle formation events occurred, producing 6 nm particles at a rate of about 1 $cm^{-3}\,s^{-1}$. Typical particle growth rates were between 6 and 7 $nm\,h^{-1}$. Ion measurements showed the typical cluster band below 2 nm, with total ion concentrations roughly between 600 and 1000 cm^{-3}. A peculiar feature of the ion measurements were heightened ion cluster concentrations during the nights before event days. At 2 nm, the formation rate of charged particles was only about 0.2 % of the total rate, pointing towards an only marginal role of ion-induced nucleation. Based on observations, a simple empirical criterion was deducted to estimate particle formation probability. Dominated by radiation and relative humidity, the criterion can predict the occurrence of particle formation with a 90 % accuracy. In a similar fashion, a reasonably accurate estimate of particle formation rates was derived. Combined, these parameters allow for a description of particle formation based on a few basic measured variables.

1 Introduction

Atmospheric aerosols play a significant role in the Earth's radiative balance. They scatter and reflect incoming sunlight (direct effect; Twomey, 1974; Charlson et al., 1992; Bellouin et al., 2008), affect cloud properties (indirect effect; Twomey, 1984, 1991; Lohmann and Feichter, 2005), and can prevent cloud formation under certain condi-

ACPD
13, 22337–22381, 2013

tions (semi-direct effect; Hansen et al., 1997; Allen and Sherwood, 2010). The IPCC Report 2007 has identified aerosols as the main uncertainty in our understanding of radiative forcing. Aerosols also affect human health and have been linked to asthma, lung cancer, and cardiovascular diseases among others (e.g. Pope and Dockery, 2006).

A central phenomenon related to atmospheric aerosols is new particle formation (atmospheric nucleation), i.e. the production of particulate matter from pre-existing vapors (secondary aerosols). New particle formation has been observed all over the world under a wide variety of conditions (Kulmala et al., 2004; Kulmala and Kerminen, 2008) which suggests that different processes may be at work. While sulfuric acid has been identified as the key vapor involved (e.g. Sipilä et al., 2010; Kerminen et al., 2010), the roles of organic vapors, ammonia/amines, air ions, and clusters are under discussion (Kulmala et al., 2013); their influence may well vary with environmental conditions. In order to monitor and understand climate change, forcing and related feedbacks, also including the role of aerosols and aerosol processes such as nucleation, Hari et al. (2009) have suggested the establishment of a global network of measurement stations.

As part of a general growing interest in environmental issues, aerosols and particle formation have seen increased research efforts in China during recent years. However, so far only few comprehensive studies have been published (e.g. Shen et al., 2011). Instead, many projects have had rather campaign character, presenting only a few weeks of observations (e.g. Gao et al., 2011; Liu et al., 2008). Also there has been a strong focus especially on Beijing (e.g. Yue et al., 2011; Gao et al., 2012; Zhang et al., 2011), but also on Hong Kong and the Pearl River Delta (e.g. Gong et al., 2010), and urban areas in general (e.g. Gao et al., 2007; Xu et al., 2011). There are few background sites, and, for example, the Yangtze River Delta (YRD), home to 100 million people, the largest conglomerate of adjacent megacities in the world, one of the motors of Chinese industrial development and a hotspot of human activity, has seen only little research activity in terms of aerosols and particle formation (e.g. Huang et al., 2013). A significant portion of the published research does not extend to particle sizes below

ACPD
13, 22337–22381, 2013

10 nm (e.g. Du et al., 2012), and no data has been published down to cluster size (ca. 1 nm).

At the western end of the Yangtze River Delta, outside the city of Nanjing, the Station for Observing Regional Processes of the Earth System (SORPES) is set up to measure mainly YRD background air masses (as opposed to Nanjing urban air). The station is designated to evolve into a "flagship station" according to the Hari et al. (2009) proposition and currently houses various aerosol, trace gas, and meteorological measurements. In this article, we present the first results from ongoing, continuous measurements of particle size distributions performed at SORPES. The measurement period spans from 18 November 2011 to 31 March 2012, forming the longest and most comprehensive data set on aerosols and related variables in the region to date. We present the first data on air ion clusters observed in China and quantify how atmospheric conditions affect new particle formation.

2 Measurement station

2.1 Site and location

SORPES-NJU is located some 20 km east of downtown Nanjing in Eastern China. The exact coordinates are 32.12° N and 118.95° E. Nanjing has a humid subtropical climate with high relative humidity during the whole year. Haze occurs frequently. In the summer, temperatures can be well above 30 °C while temperatures somewhat below 0 °C are not uncommon during the winter months. The station is situated on a hill rising about 40 m above its surroundings, overlooking the new campus of Nanjing University which can be considered a suburban environment. With prevailing easterly winds throughout the year, the station mainly monitors YRD background air. The station currently measures aerosols, trace gases, fluxes, radiation, and meteorological data. A detailed account of the measurement station and its intents and purposes is presented in Ding et al. (2013a).

ACPD
13, 22337–22381, 2013

The site is located in a relatively rural environment with few local emission sources within 2–3 km. There is a large petro-industrial zone located about 5–10 km northwest of the site, but because of prevailing winds from the east (Ding et al., 2013a) and some small hills between this zone and the site, these air masses are rarely transported to the site. Besides these, an important local source of PM worthwhile to be mentioned is the wind-blow road dust. As there were intensive construction activities in the campus and 2–5 km in the east and transport of soil and stones often made the road very dirty and that dust can easily be blown by strong wind and vehicle-introduced turbulence, especially in the dry winter seasons. These activities generally caused a pollution of coarse mode particles. The mainly regional sources located in the East and South-east direction with a distance up to 300 km, with many factories/power plants located along the Yangtze river and more developed cities, such as Shanghai, Suzhou, Wuxi, Changzhou and Nanjing city clusters, located in the South side of the Yangtze river.

2.2 Instrumentation and measurements

The central aerosol instrumentation used in this study consists of an air ion spectrometer (AIS) and a differential mobility particle sizer (DMPS, built at Helsinki University). Similar combinations have previously been successfully used in the study of atmospheric nucleation (e.g. Manninen et al., 2010).

The AIS consists of two parallel DMAs (differential mobility analyzer) for negative and positive air ions, respectively. The inner walls of the DMAs are outfitted with electrometers allowing for a direct detection of the currents caused by ion impact on the wall. The AIS detects ions between 0.8 and 42 nm (mobility) diameter in 21 channels (size ranges) per DMA. During the measurements presented here, the AIS was operated in a 2 plus 1 min cycle (2 min sampling plus 1 min background determination), making for a time resolution of 3 min. To minimize data deterioration caused by the deposition of particles on the inner surfaces of the DMAs, both analyzers had to be cleaned thoroughly at least once per month. Deposition of dirt onto the nets inside the venturi flow tubes can lower the flow rate and thus effect the operation of the mobility analyzers.

ACPD
13, 22337–22381, 2013

Those nets were cleaned at least once per week. Poor quality data was excluded from further numerical analysis. The AIS in detail is described in Mirme et al. (2007).

The differential mobility particle sizer used in this study can be described as a "virtual twin" DMPS, i.e. a single DMPS run at two different flow rates to extend its size range (Salma et al., 2011). The inlet in equipped with an impactor of 2.5 µm cutoff diameter to avoid the deposition of large particles inside the instrument. The sample is dried using nafion tubes, and equilibrium charge is ensured by two americium 241 sources (each about 37 kBq). Particles are counted by a TSI 3772 butanol CPC (condensation particle counter). The DMPS provides the number size distribution between 6 and 800 nm mobility diameter. The time resolution is 10 min.

Besides aerosol and air ion size distribution data, this study also uses the following data: $PM_{2.5}$, global radiation, temperature, wind speed and direction, ozone concentration, and SO_2 concentration. All instruments used are listed in Table 1 and more detailed descriptions of the instrumentations were given by Ding et al. (2013a).

2.3 Data analysis

The analysis of the particle size distribution data in general and particle formation events in particular follows the procedures described in great detail by Kulmala et al. (2012). The growth rate GR of a particle population can be expressed as

$$\mathrm{GR} = \frac{\mathrm{d}d_\mathrm{p}}{\mathrm{d}t} = \frac{\Delta d_\mathrm{p}}{\Delta t} = \frac{d_{\mathrm{p}2} - d_{\mathrm{p}1}}{t_2 - t_1} \quad (1)$$

where diameters $d_{\mathrm{p}1}$ and $d_{\mathrm{p}2}$ describe the particle population at times t_1 and t_2. In the framework of the Kulmala et al. (2012) Protocol, the maximum concentration method was used in which the center of the measured size bin is used as the representative diameter. The formation rate J_{d_p} of particles of diameter d_p is:

$$J_{d_\mathrm{p}} = \frac{\mathrm{d}N_{d_\mathrm{p}}}{\mathrm{d}t} + \mathrm{CoagS}_{d_\mathrm{p}} \cdot N_{d_\mathrm{p}} + \frac{\mathrm{GR}}{\Delta d_\mathrm{p}} \cdot N_{d_\mathrm{p}} + S_\mathrm{losses} \quad (2)$$

ACPD
13, 22337–22381, 2013

Here, CoagS_{d_p} is the coagulation sink for particles between d_p and $d_p + \Delta d_p$, GR is their respective growth rate, and S_{losses} covers additional loss processes. For the treatment of ions, additional terms are necessary to include recombination and charging by smaller particles. The actual nucleation rate, i.e. the formation rate of critical clusters, can be deducted from the apparent formation rate using the condensation or coagulation sink and (an estimate of) the growth rate between the relevant sizes as parameters (Lehtinen et al., 2007). Also values such as the concentration of available vapor or the vapor source rate can be extracted from size distribution data (see Kulmala et al., 2012 for further details).

The most comprehensive sulfuric acid proxy to date has been constructed by Mikkonen et al. (2011) who compared data collected at seven sites in Europe and North America. They have determined a proxy for each site as well as a universal proxy that is thought to be valid elsewhere as well. Their universal proxy has the form

$$[\mathrm{H_2SO_4}]_{\mathrm{universal}} = 8.21 \times 10^{-3} \cdot k \cdot \mathrm{Radiation}^{1.00} \cdot [\mathrm{SO_2}]^{0.62} \cdot (\mathrm{CS} \cdot \mathrm{RH})^{-0.13} \quad (3)$$

where k is the reaction rate constant and dependent on temperature. Radiation, $[\mathrm{SO_2}]$, CS, and RH are (global) radiation, $\mathrm{SO_2}$ concentration, condensational sink, and relative humidity, respectively. Among the sites considered by Mikkonen et al. (2011) is the city of Atlanta which has similar climate conditions as Nanjing. Therefore we have also used the best Atlanta proxy to gain an estimate of sulfuric acid concentrations. The Atlanta proxy has the following form:

$$[\mathrm{H_2SO_4}]_{\mathrm{Atlanta}} = 1.30 \times 10^{-1} \cdot k \cdot \mathrm{Radiation}^{1.10} \cdot [\mathrm{SO_2}]^{0.69} \cdot \mathrm{CS}^{-0.53} \cdot \mathrm{RH}^{-1.92} \quad (4)$$

To gain more insight into the relation of incoming air masses and nucleation behavior, we used the Hybrid Single-Particle Lagrangian Integrated Trajectory (HYSPLIT) dispersion model (Draxler and Hess, 1998) following a method described by Ding et al. (2013b). For each day when nucleation was observed, the model was run 1-day backwardly with 3000 particles released 100 m over the measurement site. Thus, a footprint retroplume was identified providing information about the origin and history of the observed air masses.

ACPD
13, 22337–22381, 2013

3 Results and discussion

3.1 Overview of the measurements

3.1.1 Meteorological conditions

The data presented in this study covers the period from the middle of November 2011 to the end of March 2012, i.e. local winter, framed by late autumn and early spring. The average mean temperature during this period was 5.2 °C, with daily averages from −3.0 to 20.2 °C. The temperature profile (Fig. 2a) was characterized by quite a regular oscillating shape indicating the passing of cold fronts. Throughout the measurement period, daily-average temperatures oscillated by as much as 10 °C within a few days. However, underlying this fluctuation, the seasonal trend was clearly visible.

The radiation (Fig. 2b) did not exhibit a clear seasonal behavior for most of the measurement period as the change in the Sun's position would suggest. The significance of this observation will be discussed in the sections related to nucleation frequency and nucleation characteristics. However, the radiation data plot quite convincingly conveys its anti-correlation with the humidity data in the same panel: high humidity suggests rain or clouds which again means less radiation at ground level. The wind direction histogram (Fig. 2c) reflects the dominance of easterly winds with the main wind direction being around 70° and almost all wind directions between 30° and 120°. This means that the station hardly ever sees pollution from downtown Nanjing in the west and the industrial zone in the northwest while air masses from the YRD occur frequently. The impact of this on aerosol characteristics and new particle formation will be discussed in the appropriate sections.

3.1.2 Aerosol characteristics

Figure 3 illustrates how air ion concentrations and modal aerosol particle concentrations depend on the wind direction. In Fig. 3a, the ion clusters represent the sum of

ACPD
13, 22337–22381, 2013

positive and negative ions below 2 nm of mobility diameter (note: generally, in this manuscript, the unqualified "ion" will always mean total ions, i.e. the sum of positive and negative ions). The nucleation mode (Fig. 3b) covers the diameter range 6 to 25 nm, the Aitken mode (Fig. 3c) the range 25 to 90 nm, and the accumulation mode (Fig. 3d) the range 90 to 800 nm.

Considering the ion clusters, the most interesting detail is the comparison to the accumulation mode in Fig. 3d. While the ion cluster concentration did not change much with the wind direction, there seemed to be some anti-correlation with accumulation mode concentrations: the accumulation mode particle number concentrations were the highest at wind directions between 60° and 180°, while ion cluster concentrations were the lowest for the same wind directions. There was also a local maximum in the ion cluster concentration between about 330° and 360° and a corresponding minimum in the accumulation mode number concentration. However, this latter feature should not be overstated as winds from that direction are rare (Fig. 2c) and statistics thus poor. In any case, the relationship between ion cluster and accumulation mode concentration can be easily enough explained with the coagulation sink due to accumulation mode particles which remove small clusters and particles.

The nucleation mode (Fig. 3b) displayed two main features. Firstly, the average nucleation mode concentrations were relatively low in the prevailing wind direction (easterly). Secondly, when the wind came from the north (0–30°), nucleation mode concentrations were almost twice as high as for the other wind directions. These observations can be interpreted as a higher nucleation probability for northern air masses and a lower nucleation probability for the other wind directions. Comparing this to the Aitken and especially the accumulation mode (Fig. 3c and d), we observe rather low concentrations in the Aitken and accumulation mode for the northern air masses. This suggests that at least part of the higher nucleation mode concentrations (i.e. higher nucleation probability) in this sector can be explained as a consequence of lower concentrations of larger particles, i.e. a lower condensation sink. In accordance with this,

ACPD
13, 22337–22381, 2013

quite large amounts of larger particles are associated with easterly winds, explaining the lack of nucleation from this direction by the same mechanism.

During the measurement period from 18 November 2011 to 31 March 2012, on average (median), a total (sum of positive and negative ions) of 770 cm^{-3} ion clusters below 2 nm diameter were observed, with the 25 and 75 percentiles being 600 and 970, respectively, in line with earlier findings that the "cluster band" below 2 nm is ever-present and subject only to relatively small fluctuations (Hirsikko et al., 2005). Between 6 and 25 nm, i.e. in what could be considered the nucleation mode, a median of 3500 cm^{-3} particles was observed, with 25 and 75 percentiles of 2100 and 6000, respectively. For the Aitken mode (25–90 nm) and the accumulation mode (90–800 nm), the median (25 and 75 percentiles) were 8500 (6100 and 11 500) and 6600 (4700 and 9100), respectively. To estimate the fraction of charged particles, we integrated ion and particle number concentrations in the instruments' overlapping region from 6 to 30 nm. For the total particle to ion ratio, we found a median value of 4.4 (percentiles 3.4 and 5.9). Table 2 lists these numbers together with the means and 5 and 95 percentiles to characterize the aerosol population more completely. Considering modal particle number concentrations, the nucleation and Aitken mode showed the largest variations, accounting for days with and without new particle formation. The range of accumulation mode concentrations, on the other hand, was not related to local phenomena but rather an indication of the pollution level of the incoming air masses. Accordingly, the median and percentiles of $PM_{2.5}$ mass concentrations (79, 47, 116 $\mu g\,m^{-3}$) quite closely followed the respective percentiles of the accumulation mode particle number concentrations.

3.2 Aerosol formation and growth

3.2.1 General characteristics

All recorded new particle formation events were of type Ib.2 (classification according to Hirsikko et al., 2007) with a noticeable gap between the cluster band (below 2 nm) and what is informally called the nucleation "banana" (Fig. 4). The growth of nucle-

ACPD
13, 22337–22381, 2013

ated particles could be observed over several hours after the initial onset of particle formation.

New particle formation was observed on 26 days during the measurement period, which makes for a nucleation probability of roughly 20 %. Nucleation occurred during all months of the measurements, with somewhat less activity during November and December (see Table 3). A pronounced "winter break", as typically seen in northern latitudes (e.g. Dal Maso et al., 2007; Asmi et al., 2011), could not be observed.

The wind direction and the origin and history of the incoming air masses have been found to play a significant role in new particle formation (Sogacheva et al., 2005; Dal Maso et al., 2007). Figure 5 summarizes the situation at the SORPES site for the measurement period. The nucleation probability was quite high (around and over 40 %) for most wind directions (Fig. 5b), while being rather low for the easterly winds (ca. between 45° and 100°). Incidentally, the direction of the low nucleation probability is also the prevailing wind direction (see Fig. 2), amounting to the total nucleation probability of about 20 % as noted earlier. Figure 5a shows the 1-day retroplumes for the nucleation event days recorded during the measurement period. It is noteworthy that events were only observed when air masses originated from the NNE half of the map (300–120° in terms of wind directions). It seems plausible that air masses from SSW typically pass over heavily polluted Nanjing and adjacent industrial areas and are therefore so saturated with particles that the high condensation sink makes new particle formation unlikely. The accumulation mode in Fig. 3d with the highest concentrations in the south supports this view. A striking feature of Fig. 5a is the "gap" to the east (ca. 100–130°). This gap is home to Shanghai, Suzhou, and Wuxi – essentially all major cities in the YRD. Ding et al. (2013a) found an important potential source contribution from this city-cluster to trace gases and aerosol mass concentrations measured at the SORPES site. Figure 5a thus states that no new particle formation was observed with air masses coming from the cities of the YRD, and high particle loads seem again the most plausible explanation. The numbers in Table 3 further stress the point. In the diameter range 10 and 100 nm (i.e. where new particles should contribute), Gao et

ACPD
13, 22337–22381, 2013

al. (2009) observed over 28 000 cm^{-3} particles at a site outside Shanghai, while we saw only 13 000 outside Nanjing. Part of this difference might well be explained with the different measurement periods, yet the theory that high pre-existing particle loads suppresses nucleation seems a more plausible explanation: between 100 and 500 nm, SORPES observed almost fourfold particle concentrations compared with the Shanghai site. Considering the prevailing easterly winds (i.e. from Shanghai and YRD), it is also fairly obvious that much of the accumulation mode observed at the SORPES site has its origin in the YRD.

The extremely low concentrations of the smallest (< 3 nm diameter) newly formed ions (see the gap in Fig. 4) make it impossible to determine a reliable estimate of the growth rate for these particles. For particles between 3 and 7 nm, AIS measurements yielded a median growth rate of 5.9 nm h^{-1} with 25 and 75-percentiles of 4.4 and 7.9 nm h^{-1}, respectively (Table 5). From 7 to 30 nm, the AIS growth rate had a median of 6.7 nm h^{-1} (percentiles 5.2 and 8.2). Based on the DMPS data, the growth rate between 6 and 30 nm was 6.9 nm h^{-1} (percentiles 6.1 and 10.9), whereas the larger particles grew almost as fast at 6.6 nm h^{-1}. These results are well within the range of observations from Europe reported, for example, by Manninen et al. (2010). In China, urban observations have typically yielded somewhat smaller means between roughly 3 and 6 nm h^{-1} (e.g. Yao et al., 2010; Du et al., 2012; Gao et al., 2012) while Wang et al. (2011) reported growth rates of up to 36 nm h^{-1} from Beijing. In suburban Shanghai, Gao et al. (2009) found a mean growth rate of 6.4 nm h^{-1} which is quite close to our values.

The observed formation rate (averaged over each nucleation event) of 6 nm particles J_6 was 0.82 cm^{-3} s^{-1} (percentiles 0.51 and 1.23). Following the method outlined by Kulmala et al. (2012), the formation rate of 2 nm-particles J_2, representing more closely the actual nucleation rate, was estimated to be 23.9 cm^{-3} s^{-1} (median value) with percentiles of 14.8 and 56.8, respectively. A comparison to other studies from China is difficult in this case because typically only the apparent formation rate has been reported as opposed to the actual nucleation rate. However, the 3 nm particle formation

ACPD
13, 22337–22381, 2013

rates of 8.0 cm^{-3} s^{-1} by Shen et al. (2011) and 3.44 cm^{-3} s^{-1} by Liu et al. (2008) as well as the 10 nm formation rates between 0.2 and 0.5 cm^{-3} s^{-1} by Du et al. (2012) would appear to be of the same order of magnitude as our values. During new particle formation events, a median number of 18 000 cm^{-3} 6 nm particles was produced (percentiles 7300 and 29 000), and the concentration of accumulation mode particles grew by 4400 cm^{-3} (percentiles 2800 and 5400). During particle formation events, the condensational sink had a median value of 0.025 s^{-1} (percentiles 0.02 and 0.03) while over the whole measurement period it was 0.04 (percentiles 0.03 and 0.055).

A comparison of J_2 and J_6 for ions and total particles (ions + neutral particles) provides insight into the role of ions in the particle formation process and also explains the gap in ion concentrations seen in Fig. 4. Table 6 shows an extremely small value of J_2 for ions that is only 0.2 % of the respective value for all particles. Manninen et al. (2010) reported corresponding values between 1 and 30 % in a comparison of various European sites. At the SORPES site, we found the ion contribution to be one or even two orders of magnitude smaller, so the neutral particle formation pathway clearly dominates. With J_2 being so small for ions, naturally also the concentration of 2 nm ions is very small, so small indeed that the color scheme in makes them virtually disappear from the example case shown in Fig. 4. The growing ratio of J_{ion} to J_{total} from 2 to 6 nm shown in the last column of Table 6 can be interpreted in such a way that the initially mostly neutral clusters take up charges during their growth to larger sizes. This also explains the gradual appearance of the so-called banana in the ion plot in Fig. 4. The process of charge exchange in a growing particle population has been explored theoretically by Kerminen et al. (2007) and using model simulations by Leppä et al. (2009).

An intriguing feature of the ion cluster behavior is shown in Fig. 6a: a small, but as we believe significant, difference in cluster ion concentrations (< 2 nm) between the event and non-event days. We can see that cluster ions had increased concentrations during the event days before the new particle formation started. It has to be noted that the peak in cluster ion concentration during event days occurred at around 04:00 LT during the

ACPD
13, 22337–22381, 2013

night, i.e. several hours before sunrise. The mechanism behind this behavior is unclear. When the new particle formation started properly (i.e. between 09:00 and 11:00 a.m. as seen in Fig. 6b), the cluster ion concentration for the event days had almost returned to the non-event level. Since the new particle formation occurred about 5–7 h after the observed peak in the cluster ion concentration, it is highly unlikely that the increased cluster ion concentrations during the night could have a direct effect on new particle formation, especially because the role of ion-induced nucleation seemed to be rather small. However, the ion cluster behavior could correlate with processes or conditions that directly or indirectly favor new particle formation.

3.2.2 Factors influencing particle formation and growth

New particle formation is closely related to the availability of sulfuric acid vapor (e.g. Sipilä et al., 2010; Kerminen et al., 2010; Kulmala et al., 2013) and thus dependent on a number of parameters central to sulfuric acid formation. These include radiation, condensational sink (as a measure of pre-existing aerosol), SO_2 concentration, and relative humidity (e.g. Petäjä et al., 2009; Mikkonen et al., 2011). Figure 7 shows the median diurnal cycles of these quantities as well as their quartile values, separated for days with and without new particle formation to provide an impression of how these quantities might influence the formation of new particles.

Radiation drives the formation of sulfuric acid, and the clear separation of the data for days with and without nucleation highlights the central role that radiation plays to make particle formation possible (Fig. 7a). The situation is almost as clear for relative humidity (RH), with new particle formation being favored by lower values of RH. This is closely related to radiation, as sunny and drier conditions typically go hand in hand. Additionally, a high relative humidity can lead to a growth of the condensation sink and thereby to haze formation which affects radiation. As a whole, however, the nature of the RH impact on particle formation differs fundamentally from the radiation case. While radiation is the actual driving force behind sulfuric acid formation, RH is mostly an indicator of favorable conditions. The median of the condensation sink in Fig. 7c clearly

ACPD
13, 22337–22381, 2013

shows that particle formation is more likely when there are fewer pre-existing aerosol particles, as would be expected. However, the quartiles point out that the separation is not very distinct, indicating that particle formation is possible also with relatively high aerosol loads.

Figure 7b shows the diurnal cycles of the SO_2 concentration, the precursor for gaseous sulfuric acid. We can see that higher SO_2 concentrations did not lead to higher nucleation probabilities but, instead, the median SO_2 concentration during event days was below that during the non-event days. While SO_2 is a precursor for sulfuric acid, it is also an indicator of pollution in general which includes particulate matter (i.e. condensational sink). Under conditions of absolutely high SO_2 concentrations at all times, the positive causal relation of SO_2 with sulfuric acid gets outweighed by the high aerosol load it also indicates. This leads to the situation depicted in Fig. 7b where, despite its actual role, higher SO_2 indicates a lower nucleation probability.

Of the observations depicted above, the behavior of radiation, condensation sink, and relative humidity can be considered globally consistent. The degree of separation between event days and non-event days may vary, and all these variables have not always been reported, yet partly similar findings have been reported from northern Finland (Vehkamäki et al., 2004), from the Korean coast (Lee et al., 2008), from Po Valley in Italy (Hamed et al., 2007) as well as from Beijing (Wu et al., 2007). The behavior with respect to SO_2, however, seems to vary largely. In Korea, the effect of SO_2 concentration on the nucleation probability was found to be positive, in the Po Valley neutral to positive, and in Beijing (as in our observations) negative. Summarizing these different results, the behavior of SO_2 appears to be the main indicator of the global differences in particle formation, reflecting the general pollution level of the respective site as well as the role and predominance of sulfuric acid in particle formation and early growth and the influence of these factors on the process of particle formation as a whole.

While sulfuric acid concentration is believed to be the key factor in new particle formation, the rather demanding sulfuric acid measurements are not routinely performed

ACPD
13, 22337–22381, 2013

and such data is therefore not generally available. To nevertheless estimate the H_2SO_4 concentration, proxies can be constructed that allow its determination based on a number of typically available measurements, such as the temperature, radiation, SO_2 concentration, condensation sink CS and relative humidity. The results for the Mikkonen et al. (2011) proxies (see Sect. 2.3), again separated for days with and without particle formation, are presented in Fig. 8. The proxies (see Eqs. 3 and 4) differ most significantly in their treatment of relative humidity. The universal proxy almost ignores its impact, while the Atlanta proxy gives it an exponent of almost −2. As we can see from Fig. 7d, the relative humidity differed significantly between the event and non-event days. As a consequence of the different RH treatment, the two proxies give significantly different estimates of sulfuric acid. The universal proxy (Fig. 8a) is essentially quite similar to the radiation data presented in Fig. 7a, whereas the Atlanta proxy shows higher values for the event days, lower values for the non-event days, and a larger variation of data as indicated by the quartiles. Interestingly, the mean value over the whole measurement period was approximately the same at 1.2×10^7 cm^{-3}. Very similar values have been measured in Atlanta. However, the treatment of RH and the stronger distinction between event and non-event days suggests that the Atlanta proxy is the more probable choice to estimate sulfuric acid concentrations in Nanjing. Nevertheless, the much higher pollution values in Nanjing (CS, $PM_{2.5}$, SO_2) underline the fact that the conditions at both sites are quite different. As the next section discusses, especially the treatment of SO_2 raises questions as to how accurately the proxies by Mikkonen et al. (2011) can capture conditions at the SORPES site, despite numerically reasonable results and generally plausible behavior of those proxies with respect to Nanjing data.

Based on size distribution data, it is possible to extract information about the amount of condensable vapors available for particle growth (Kulmala et al., 2012). This can be compared with the sulfuric acid concentrations estimated by the proxy to estimate what fraction of the particle growth was caused by sulfuric acid. For the universal proxy by Mikkonen et al. (2011), we found a mean of 0.47 for the sulfuric acid fraction of the growth with the standard deviation being equal to 0.29 and the median equal to 0.37

ACPD
13, 22337–22381, 2013

with quartiles of 0.22 and 0.65. As seen above, the Atlanta proxy predicted higher sulfuric acid concentrations and more variation. Accordingly, the mean fraction of growth due to sulfuric acid using the Atlanta proxy was 0.73 with a standard deviation of 0.56, a median of 0.55 and quartiles of 0.24 and 1.11. Clearly, while generally behaving "better", the Atlanta proxy overestimates sulfuric acid concentrations at least in some cases. Nevertheless, even the conservative estimate of the universal proxy predicts mean sulfuric acid contributions to early particle growth of almost 50 %, highlighting the important role of sulfuric acid in polluted environments and further stressing the need for detailed research into this subject. Previous investigations of the role of sulfuric acid in particle growth have shown that it depends largely on the availability of SO_2, i.e. the pollution level. At remote and less polluted locations, sulfuric acid has been estimated to contribute below 20 % (e.g. Fiedler et al., 2005; Boy et al., 2005), whereas Yue et al. (2010) reported a 34–45 % contribution for Beijing and Gao et al. (2011) a 68.3 % contribution for urban Lanzhou. Our results fall between these other values from China and thus underline that the details of the particle formation process vary significantly even within the country.

3.2.3 Predictions

Just as the sulfuric acid proxy is a useful tool in the absence of sulfuric acid measurements, a parameter to predict whether nucleation takes place or not based on a number of key variables can be a useful tool for e.g. modeling purposes. McMurry et al. (2005) developed such a parameter (which they named new particle formation criterion) and tested it for the conditions in Atlanta. Using the sulfuric acid proxy for Atlanta, this criterion can be rewritten as

$$L' \sim \frac{\mathrm{CS}^{1.53} \cdot \mathrm{RH}^{1.92}}{\mathrm{Radiation}^{1.10} \cdot [\mathrm{SO_2}]^{0.69} \cdot T^{0.5}} \quad (5)$$

If L' is smaller than a certain threshold value, particle formation should be observed. Considering the application of this parameter to the Nanjing conditions, we notice that

ACPD
13, 22337–22381, 2013

Eq. (5) is actually not consistent with the data presented in Fig. 7. The equation treats SO_2 as a factor favoring particle formation, while Fig. 7b clearly shows that event days show lower SO_2 concentrations than non-event days. Moreover, no correlation could be observed between temperature T and nucleation probability (not shown) in Nanjing. Thus, a parameter reflecting observations at the SORPES station should have the following form:

$$L'' \sim \frac{CS^a \cdot [SO_2]^b \cdot RH^c}{\text{Radiation}^d} \quad (6)$$

where a, b, c, and d are fitting parameters having positive values. These parameters can then be optimized in such a way that the overlap between data points representing event and non-event days becomes as small as possible. For the measurement period, the smallest overlap found was 10 % which means that the lowest 10 % of the non-event day data points and the highest 10 % of the event day data points overlapped. For the best separation, the values of the fitting parameters were $a = 1.6$, $b = 0.6$, $c = 5.6$, and $d = 3.5$ (see Fig. 9a). At face value, these exponents are well within reason. The exponent for SO_2 is quite small, indicating the dual role of SO_2 as discussed above and highlighting that, ultimately, actual SO_2 concentrations are of minor importance under heavily polluted conditions. The remaining variables CS, RH, and radiation and their exponents roughly represent $[H_2SO_4]^{-3}$ (see Eq. 4) only without SO_2, again pointing out that the role of SO_2 in the sulfuric acid proxy is the main source of uncertainty. Linking our empirical criterion to $[H_2SO_4]^{-3}$ is a significant departure from the McMurry criterion where sulfuric acid had the exponent −1. However, while separating events from non-events very well, it has to be understood that these purely empirical exponents do not necessarily provide deeper insight into the formation process. The reason for this lies in the very nature of the optimization process in which they were found. This process was not concerned with *typical* behavior. Instead, the exponents are likely to be significantly determined by data points which are far away from median values. How-

ACPD
13, 22337–22381, 2013

ever, at 90 % separation, this empirical criterion is an easy and reliable way to predict a main parameter of particle formation.

Similar to the above approaches for sulfuric acid and particle formation criterion, an attempt can be made to describe the particle formation rate in terms of the same parameters:

$$J_{6,\mathrm{theo}} = k_{\mathrm{NPF}} \cdot \mathrm{Radiation}^{a}[\mathrm{SO_2}]^{b} \cdot \mathrm{RH}^{c} \cdot \mathrm{CS}^{d}. \quad (7)$$

In this equation, k_{NPF} is a constant factor, $J_{6,\mathrm{theo}}$ is given in units $\mathrm{cm}^{-3}\,\mathrm{s}^{-1}$, radiation is given in Wm^{-2}, $[\mathrm{SO_2}]$ is given in ppb, RH is given in %, and CS is given in s^{-1}. The pre-factor and the exponents a, b, c, and d can then be optimized in such a way (allowing for positive and negative values for all exponents) that $J_{6,\mathrm{theo}}$ is as close to the measured formation rate $J_{6,\mathrm{meas}}$ as possible (least squares fit). The best fit obtained this way gave $k_{\mathrm{NPF}} = 2.75 \times 10^{-13}$, $a = 3.0$, $b = 1.0$, $c = 0.3$, and $d = -1.9$. With these values, theoretical and measured formation rates can be matched with $R^2 = 0.77$ (see Fig. 9b). The temperature was not included in Eq. (7) because our tests showed that including this parameter did not produce a better fit. Just as with the particle formation criterion (Eq. 6), the nucleation rate again shows the exponents for radiation and condensational sink with a factor of roughly 3 when compared to the Atlanta sulfuric acid proxy. Compared with the criterion for occurrence of nucleation (Eq. 6) and sulfuric acid proxy (Eq. 4), RH seemed to play almost no role in actual particle formation rate, indicating that its role in Eq. (6) is to act first and foremost as an indicator of general conditions with relation to potential particle formation. $\mathrm{SO_2}$, with a different subset of data, has changed the sign of its exponent. In short, the analysis shows formation to be determined by radiation as the main driving force and condensation sink as the main obstacle. This parameterization provides a relatively simple way to predict formation rates. Given actual measurements of sulfuric acid (instead of a proxy) and a lower aerosol detection limit, this analysis can also provide a link between sulfuric acid and nucleation rate of the form $J \sim [\mathrm{H_2SO_4}]^{n}$ which provides insight into the formation mechanism. With the current state of instrumentation, the tentative $n \approx 3$ has to

ACPD
13, 22337–22381, 2013

be considered as rather speculative and unreliable, even if recent results by Wang et al. (2011) show that, in China, *n* can significantly exceed the typical range between 1 (cluster activation) and 2 (kinetic nucleation).

4 Summary and conclusions

The Station for Observing Regional Processes of the Earth System at Nanjing University (SORPES-NJU) is set up to measure atmospheric processes continuously and on a long-term basis. As part of the stations operations, aerosol and air ion measurements started in the end of 2011. The first results from those measurements were presented in this paper.

From the middle of November 2011 to the end of March 2012, an air ion spectrometer (AIS) and a differential mobility particle sizer (DMPS) monitored the air ion (0.8–42 nm) and aerosol (6–800 nm) populations at a site outside Nanjing in the Yangtze River Delta in eastern China. For the total particle concentration, the measured mean value of 2.3×10^4 cm^{-3} is of the same order of magnitude as similar observations in China, Europe, and the US (see Table 6). Interestingly, a much larger fraction of the total particle number was due to larger particles when comparing Nanjing to other (urban) locations, resulting in high $PM_{2.5}$ loads with a mean value of 90 µg m^{-3}, well above the annual national limit of 35 µg m^{-3} and even above the daily average limit of 75 µg m^{-3}. Observations give reason to assume that high accumulation mode concentrations are mainly imported from pollution sources east of Nanjing, i.e. from the YRD. Accordingly, not a single particle formation event was observed when air masses came in from the YRD.

New particle formation was observed on 26 days, resulting in a nucleation probability of almost 20 %. Typical growth rates of newly-formed particles were between 6 and 7 nm h^{-1}, which falls well within the range observed for example in Europe (e.g. Manninen et al., 2010). An average nucleation event day produced more than 4000 cm^{-3} new particles into the accumulation mode. A peculiar feature of new particle formation

ACPD
13, 22337–22381, 2013

at the site is a heightened ion cluster concentration during the night prior to the onset of nucleation. The mechanism behind this observation is unclear. A typical feature of nucleation events observed at the SORPES site was an apparent gap between the cluster ion band and aerosol ions. Closer investigation of this phenomenon showed that ion concentrations in this regime were extremely small. The data shows that only very few charged particles were formed in nucleation and that newly-formed particles were mostly neutral and acquire a charge only during their growth. Of all newly formed 2-nm particles, a mere 0.2 % was estimated to carry a charge, indicating that ion-induced nucleation plays a very marginal role at the site.

A comparison of conditions between the nucleation event and non-event days showed that radiation and relative humidity are the most decisive factors while the condensational sink has less impact. While SO_2 is necessary for sulfuric acid formation, high SO_2 concentrations did not coincide with particle formation. Instead, the role of SO_2 as a pollution indicator outweighed its active role as a sulfuric acid precursor. Based on these observations, an empirical particle formation criterion was developed that predicted the occurrence of new particle formation with an accuracy of 90 %. This criterion is largely determined by radiation and relative humidity, with SO_2 concentration and condensation sink having much less impact, just as the analysis of the single variables suggested. Similarly, the formation rate of 6 nm particles, J_6, was parameterized based on observations. For J_6, radiation and condensational sink were the most important parameters, while the relative humidity could almost be neglected.

While the data presented here are the most comprehensive study on aerosols and nucleation in the Yangtze River Delta and while they illustrate the power of integrated atmospheric measurements, they also stress the need for more observations. Long-term seasonal cycles need to be established, with respect to aerosols in general as well as to nucleation and its conditions to quantify the behavior of the aerosol population at the site. The pre-nucleation behavior of ion clusters needs to be verified and further analyzed. The role of ion-induced nucleation must be studied further. Long-term observations are necessary to improve the predictive quality of our particle formation

ACPD
13, 22337–22381, 2013

criterion and formation rate parameterization. To gain detailed insight into nucleation, sulfuric acid measurements are necessary as are measurements of neutral particles down to smaller sizes.

With its choice of location, the SORPES station takes a step away from the urban bias in Chinese aerosol research. The station's air ion measurements allow the direct observation of nucleation and thus extend the previous observation range in China and Asia. Besides individual findings such as, for example, the role of ions in nucleation, these early results can be summarized by two major observations. First, results from Europe and North America cannot simply be applied globally. The role of sulfuric acid, its contribution to the formation and growth, its expression through proxies, the role of ions – these are just some of the major areas where we found differences. Secondly, much variation with respect to aerosols and particle formation can be found within China: aerosol population characteristics differ significantly even between Nanjing and Shanghai, two cities merely 300 km apart. To understand and quantify aerosols and their formation in China and Asia (and ultimately globally), much more research is necessary, especially comprehensive long-term measurements in strategic locations.

Acknowledgements. This work was funded by the National Basic Research Program 973 Project of China (2010CB428500), National Natural Science Foundation of China (No. 41275129/D0510), the Academy of Finland projects (1118615, 139656), and the European Commission via ERC Advanced Grant ATM-NUCLE. The SORPES-NJU stations were supported by the 985 program and the Fundamental Research Funds for Central Universities in China. We appreciate the contribution of Longfei Zheng, Yuning Xie, Longshan Jin, and Zhen Peng in the maintenance of the trace gases and meteorological instruments at the station.

ACPD
13, 22337–22381, 2013

References

Allen, R. J. and Sherwood, S. C.: Aerosol-cloud semi-direct effect and land-sea temperature contrast in a GCM, Geophys. Res. Lett., 37, L07702, doi:10.1029/2010GL042759, 2010.

Asmi, E., Kivekäs, N., Kerminen, V.-M., Komppula, M., Hyvärinen, A.-P., Hatakka, J., Viisanen, Y., and Lihavainen, H.: Secondary new particle formation in Northern Finland Pallas site between the years 2000 and 2010, Atmos. Chem. Phys., 11, 12959–12972, doi:10.5194/acp-11-12959-2011, 2011.

Bellouin, N., Jones, A., Haywood, J., and Christopher, S. A.: Updated estimate of aerosol direct radiative forcing from satellite observations and comparison against the Hadley Centre climate model, J. Geophys. Res.-Atmos., 113, D10205, doi:10.1029/2007JD009385, 2008.

Boy, M., Kulmala, M., Ruuskanen, T. M., Pihlatie, M., Reissell, A., Aalto, P. P., Keronen, P., Dal Maso, M., Hellen, H., Hakola, H., Jansson, R., Hanke, M., and Arnold, F.: Sulphuric acid closure and contribution to nucleation mode particle growth, Atmos. Chem. Phys., 5, 863–878, doi:10.5194/acp-5-863-2005, 2005.

Charlson, R. J., Schwartz, S. E., Hales, J. M., Cess, R. D., Coakley Jr., J. A., Hansen, J. E., and Hoffman, D. J.: Climate forcing by anthropogenic aerosols, Science, 255, 423–430, doi:10.1126/science.255.5043.423, 1992.

Dal Maso, M., Kulmala, M., Lehtinen, K. E. J., Mäkelä, J. M., Aalto, P. P., and O'Dowd, C. D.: Condensation and coagulation sinks and formation of nucleation mode particles in coastal and boreal forest boundary layers, J. Geophys. Res.-Atmos., 107, 8097, doi:10.1029/2001JD001053, 2002.

Dal Maso, M., Kulmala, M., Riipinen, I., Wagner, R., Hussein, T., Aalto, P. P., and Lehtinen, K. E. J.: Formation and growth of fresh atmospheric aerosols: eight years of aerosol size distribution data from SMEAR II, Hyytiälä, Finland, Boreal Environ. Res., 10, 323–336, 2005.

Dal Maso, M., Sogacheva, L., Aalto, P. P., Riipinen, I., Komppula, M., Tunved, P., Korhonen, L., Suur-Uski, V., Hirsikko, A., Kurtén, T., Kerminen, V.-M., Lihavainen, H., Viisanen, Y., Hansson, H.-C., and Kulmala, M.: Aerosol size distribution measurements at four Nordic field stations: identification, analysis and trajectory analysis of new particle formation bursts, Tellus B, 59, 350–361, doi:10.1111/j.1600-0889.2007.00267.x, 2007.

Dal Maso, M., Hari, P., and Kulmala, M.: Spring recovery of photosynthesis and atmospheric particle formation, Boreal Environ. Res., 14, 711–721, 2009.

ACPD
13, 22337–22381, 2013

Ding, A. J., Fu, C. B., Yang, X. Q., Sun, J. N., Zheng, L. F., Xie, Y. N., Herrmann, E., Nie, W., Petäjä, T., Kerminen, V.-M., and Kulmala, M.: Ozone and fine particle in the western Yangtze River Delta: an overview of 1 yr data at the SORPES station, Atmos. Chem. Phys., 13, 5813–5830, doi:10.5194/acp-13-5813-2013, 2013a.

Ding, A. J., Wang, T., and Fu, C. B.: Transport characteristics and origins of carbon monoxide and ozone transported to Hong Kong, South China, J. Geophys. Res., doi:10.1002/jgrd.50714, in press, 2013b.

Draxler, R. R. and Hess, G. D.: An Overview of the HYSPLIT_4 Modeling System for Trajectories, Dispersion, and Deposition, Aust. Meteor. Mag., 47, 295–308, 1998.

Du, J. F., Cheng, T. T., Zhang, M., Chen, J. M., He, Q. S., Wang, X. M., Zhang, R. J., Tao, J., Huang, G. H., Li, X., and Zha, S. P.: Aerosol Size Spectra and Particle Formation Events at Urban Shanghai in Eastern China, Aerosol Air Qual. Res., 12, 1362–1372, doi:10.4209/aaqr.2011.12.0230, 2012.

Fiedler, V., Dal Maso, M., Boy, M., Aufmhoff, H., Hoffmann, J., Schuck, T., Birmili, W., Hanke, M., Uecker, J., Arnold, F., and Kulmala, M.: The contribution of sulphuric acid to atmospheric particle formation and growth: a comparison between boundary layers in Northern and Central Europe, Atmos. Chem. Phys., 5, 1773–1785, doi:10.5194/acp-5-1773-2005, 2005.

Gao, J., Wang J., Cheng, S. H., Xue, L. K., Yan, H. Z., Hou L. J., Jiang, Y. Q., and Wang, W. X.: Number concentration and size distributions of submicron particles in Jinan urban area: Characteristics in summer and winter, J. Environ. Sci., 19, 1466–1473, 2007.

Gao, J., Wang, T., Zhou, X. H., Wu, W., and Wang, W. X.: Measurement of aerosol number size distributions in the Yangtze River Delta in China: Formation and growth of particles under polluted conditions, Atmos. Environ., 43, 829–836, doi:10.1016/j.atmosenv.2008.10.046, 2009.

Gao, J., Chai, F. H., Wang, T., and Wang, W. X.: Particle number size distribution and new particle formation (NPF) in Lanzhou, Western China, Particuology, 9, 611–618, doi:10.1016/j.partic.2011.06.008, 2011.

Gao, J., Chai, F. H., Wang, T., Wang, S. L., and Wang, W. X.: Particle number size distribution and new particle formation: New characteristics during the special pollution control period in Beijing, J. Environ. Sci., 24, 14–21, doi:10.1016/S1001-0742(11)60725-0, 2012.

Gong, Y. G., Hu, M., Cheng, Y. F., Su, H., Yue, D. L., Liu, F., Wiedensohler, A., Wang, Z. B., Kalesse, H., Liu, S., Wu, Z. J., Xiao, K. T., Mi, P. C., and Zhang, Y. H.: Competition of

ACPD
13, 22337–22381, 2013

coagulation sink and source rate: New particle formation in the Pearl River Delta of China, Atmos. Environ., 44, 3278–3285, doi:10.1016/j.atmosenv.2010.05.049, 2010.
Gu, L. H., Baldocchi, D., Verma, S. B., Black, T. A., Vesala, T., Falge, E. M., and Dowty, P. R.: Advantages of diffuse radiation for terrestrial ecosystem productivity, J. Geophys. Res.-Atmos., 107, 4050, doi:10.1029/2001JD001242, 2002.
Hamed, A., Joutsensaari, J., Mikkonen, S., Sogacheva, L., Dal Maso, M., Kulmala, M., Cavalli, F., Fuzzi, S., Facchini, M. C., Decesari, S., Mircea, M., Lehtinen, K. E. J., and Laaksonen, A.: Nucleation and growth of new particles in Po Valley, Italy. Atmos. Chem. Phys., 7, 355–376, doi:10.5194/acp-7-355-2007, 2007.
Hansen J., Sato M., and Ruedy, R.: Radiative forcing and climate response, J. Geophys. Res., 102, 6831–6864, doi:10.1029/96JD03436, 1997.
Hari, P., Andreae, M. O., Kabat, P., and Kulmala, M.: A comprehensive network of measuring stations to monitor climate change, Boreal Environ. Res., 14, 442–446, 2009.
Hirsikko, A., Laakso, L., Hõrrak, U., Aalto, P. P., Kerminen, V.-M., and Kulmala, M.: Annual and size dependent variation of growth rates and ion concentrations in boreal forest, Boreal Environ. Res., 10, 357–369, 2005.
Hirsikko, A., Bergman, T., Laakso, L., Dal Maso, M., Riipinen, I., Hrrak, U., and Kulmala, M.: Identification and classification of the formation of intermediate ions measured in boreal forest, Atmos. Chem. Phys., 7, 201–210, doi:10.5194/acp-7-201-2007, 2007.
Huang, X. F., Xue, L., Tian, X. D., Shao, W. W., Sun, T. L., Gong, Z. H., Ju, W. W., Jiang, B., Hu, M., and He, L. Y.: Highly time-resolved carbonaceous aerosol characterization in Yangtze River Delta of China: Composition, mixing state and secondary formation, Atmos. Environ., 64, 200–207, doi:10.1016/j.atmosenv.2012.09.059, 2013.
IPCC 2007: Climate Change 2007: The Physical Science Basis - Contribution of Working Group I to the Fourth Assessment Report of the Intergovernmental Panel on Climate Change, edited by: Solomon, S., Qin, D., Manning, M., Chen, Z., Marquis, M., Averyt, K. B., Tignor, M., and Miller, H. L., Cambridge University Press, Cambridge, United Kingdom and New York, NY, USA, 2007.
Kerminen, V.-M., Anttila, T., Petäjä, T., Laakso, L., Gagné, S., Lehtinen, K. E. J., and Kulmala, M.: Charging state of the atmospheric nucleation mode: implications for separating neutral and ion-induced nucleation, J. Geophys. Res., 112, D21205, doi:10.1029/2007JD008649, 2007.

ACPD
13, 22337–22381, 2013

Kerminen, V.-M., Petäjä, T., Manninen, H. E., Paasonen, P., Nieminen, T., Sipilä, M., Junninen, H., Ehn, M., Gagne, S., Laakso, L., Riipinen, I., Vehkamäki, H., Kurten, T., Ortega, I. K., Dal Maso, M., Brus, D., Hyvärinen, A., Lihavainen, H., Leppä, J., Lehtinen, K. E. J., Mirme, A., Mirme, S., Horrak, U., Berndt, T., Stratmann, F., Birmili, W., Wiedensohler, A., Metzger, A., Dommen, J., Baltensperger, U., Kiendler-Scharr, A., Mentel, T. F., Wildt, J.,Winkler, P. M., Wagner, P. E., Petzold, A., Minikin, A., Plass-Dülmer, C., Pöschl, U., Laaksonen, A., and Kulmala, M.: Atmospheric nucleation: highlights of the EUCAARI project and future directions, Atmos. Chem. Phys., 10, 10829–10848, doi:10.5194/acp-10-10829-2010, 2010.

Kulmala, M.: How particles nucleate and grow, Science, 302, 1000–1001, doi:10.1126/science.1090848, 2003.

Kulmala, M. and Kerminen, V.-M.: On the formation and growth of atmospheric nanoparticles, Atmos. Res., 90, 132–150, doi:10.1016/j.atmosres.2008.01.005, 2008.

Kulmala, M., Vehkamäki, H., Petäjä, T., Dal Maso, M., Lauri, A., Kerminen, V.-M., Birmili, W. and McMurry, P. H.: Formation and growth rates of ultrafine atmospheric particles: A review of observations, J. Aerosol Sci., 35, 143–176, doi:10.1016/j.jaerosci.2003.10.003, 2004.

Kulmala, M., Petäjä, T., Nieminen, T., Sipilä, M., Manninen, H. E., Lehtipalo, K., Dal Maso, M., Aalto, P. P., Junninen, H., Paasonen, P., Riipinen, I., Lehtinen, K. E. J., Laaksonen, A., and Kerminen, V.-M.: Measurement of the nucleation of atmospheric aerosol particles, Nat. Protoc., 7, 1651–1667, doi:10.1038/nprot.2012.091, 2012.

Kulmala, M., Kontkanen, J., Junninen, H., Lehtipalo, K., Manninen, H. E., Nieminen, T., Petäjä, T., Sipilä, M., Schobesberger, S., Rantala, P., Franchin, A., Jokinen, T., Järvinen, E., Äijälä, M., Kangasluoma, J., Hakala, J., Aalto, P. P., Paasonen, P., Mikkilä, J., Vanhanen, J., Aalto, J., Hakola, H., Makkonen, U., Ruuskanen, T., Mauldin III, R. L., Duplissy, J., Vehkamäki, H., Bäck, J., Kortelainen, A., Riipinen, I., Kurtén, T., Johnston, M. V., Smith, J. N., Ehn, M., Mentel, T. F., Lehtinen, K. E. J., Laaksonen, A., Kerminen, V.-M., and Worsnop, D. R.: Direct Observations of Atmospheric Aerosol Nucleation, Science, 339, 943–946, doi:10.1126/science.1227385, 2013.

Lee, Y.-G., Lee, H.-W., Kim, M.-S., Choi, C. Y., and Kim, J.: Characteristics of particle formation events in the coastal region of Korea in 2005, Atmos. Environ., 42, 3729–3739, doi:10.1016/j.atmosenv.2007.12.064, 2008.

Leppä, J., Kerminen, V.-M., Laakso, L., Korhonen, H., Lehtinen, K. E. J., Gagne, S., Manninen, H. E., Nieminen, T., and Kulmala, M.: Ion-UHMA: a model for simulating the dynamics of neutral and charged aerosol particles, Boreal Environ. Res., 14, 559–575, 2009.

ACPD
13, 22337–22381, 2013

Lehtinen, K. E. J., Dal Maso, M., Kulmala, M. and Kerminen, V.-M.: Estimating nucleation rates from apparent particle formation rates and vice-versa: Revised formulation of the Kerminen-Kulmala equation, J. Aerosol Sci., 38, 988–994, doi:10.1016/j.jaerosci.2007.06.009, 2007.

Liu, S., Hua, M., Wu, Z. J., Wehner, B., Wiedensohler, A., and Cheng, Y. F.: Aerosol number size distribution and new particle formation at a rural/coastal site in Pearl River Delta (PRD) of China, Atmos. Environ., 42, 6275–6283, doi:10.1016/j.atmosenv.2008.01.063, 2008.

Lohmann, U. and Feichter, J.: Global indirect aerosol effects: a review, Atmos. Chem. Phys., 5, 715–737, doi:10.5194/acp-5-715-2005, 2005.

Manninen, H. E., Nieminen, T., Asmi, E., Gagné, S., Häkkinen, S., Lehtipalo, K., Aalto, P. P., Vana, M., Mirme, A., Mirme, S., Hõrrak, U., Plass-Dülmer, C., Stange, G., Kiss, G., Hoffer, A., Törö, N., Moerman, M., Henzing, B., de Leeuw, G., Brinkenberg, M., Kouvarakis, G. N., Bougiatioti, A., Mihalopoulos, N., O'Dowd, C., Ceburnis, D., Arneth, A., Svenningsson, B., Swietlicki, E., Tarozzi, L., Decesari, S., Facchini, M. C., Birmili, W., Sonntag, A., Wiedensohler, A., Boulon, J., Sellegri, K., Laj, P., Gysel, M., Bukowiecki, N., Weingartner, E., Wehrle, G., Laaksonen, A., Hamed, A., Joutsensaari, J., Petäjä, T., Kerminen, V.-M., and Kulmala, M.: EUCAARI ion spectrometer measurements at 12 European sites – analysis of new particle formation events, Atmos. Chem. Phys., 10, 7907–7927, doi:10.5194/acp-10-7907-2010, 2010.

Matsui, H., Koike, M., Kondo, Y., Takegawa, N., Wiedensohler, A., Fast, J. D., and Zaveri, R. A.: Impact of new particle formation on the concentrations of aerosols and cloud condensation nuclei around Beijing, J. Geophys. Res., 116, D19208, doi:10.1029/2011JD016025, 2011.

McMurry, P. H., Fink, M., Sakurai, H., Stolzenburg, M. R., Mauldin, R. L., Smith, J., Eisele, F., Moore, K., Sjostedt, S., Tanner, D., Huey, L. G., Nowak, J. B., Edgerton, E., and Voisin, D.: A criterion for new particle formation in the sulfur-rich Atlanta atmosphere, J. Geophys. Res.-Atmos., 110, D22S02, doi:10.1029/2005JD005901, 2005.

Mikkonen, S., Romakkaniemi, S., Smith, J. N., Korhonen, H., Petäjä, T., Plass-Duelmer, C., Boy, M., McMurry, P. H., Lehtinen, K. E. J., Joutsensaari, J., Hamed, A., Mauldin III, R. L., Birmili, W., Spindler, G., Arnold, F., Kulmala, M., and Laaksonen, A.: A statistical proxy for sulphuric acid concentration. Atmos. Chem. Phys., 11, 11319–11334, doi:10.5194/acp-11-11319-2011, 2011.

Mirme, A., Tamm, A., Mordas, G., Vana, M., Uin, J., Mirme, S., Bernotas, T., Laakso, L., Hirsikko, A., and Kulmala, M.: A wide-range multi-channel Air Ion Spectrometer, Boreal Environ. Res., 12, 247–264, 2007.

ACPD
13, 22337–22381, 2013

Petäjä, T., Mauldin, III, R. L., Kosciuch, E., McGrath, J., Nieminen, T., Paasonen, P., Boy, M., Adamov, A., Kotiaho, T., and Kulmala, M.: Sulfuric acid and OH concentrations in a boreal forest site, Atmos. Chem. Phys., 9, 7435–7448, doi:10.5194/acp-9-7435-2009, 2009.

Pope, C. A. and Dockery, D. W.: Health effects of fine particulate air pollution: Lines that connect, J. Air Waste Manage., 56, 709–742, 2006.

Ruuskanen, J., Tuch, T., Ten Brink, H., Peters, A., Khystov, A., Mirme, A., Kos, G. P. A., Brunekreef, B., Wichmann, H. E., Buzorius, G., Vallius, M., Kreyling, W. G., and Pekkanen, J.: Concentrations of ultrafine, fine and $PM_{2.5}$ particles in three European cities, Atmos. Environ., 35, 3729–3738, doi:10.1016/S1352-2310(00)00373-3, 2001.

Salma, I., Borsós, T., Weidinger, T., Aalto, P. P., Hussein, T., Dal Maso, M., and Kulmala, M.: Production, growth and properties of ultrafine atmospheric aerosol particles in an urban environment, Atmos. Chem. Phys., 11, 1339–1353, doi:10.5194/acp-11-1339-2011, 2011.

Shen, X. J., Sun, J. Y., Zhang, Y. M., Wehner, B., Nowak, A., Tuch, T., Zhang, X. C., Wang, T. T., Zhou, H. G., Zhang, X. L., Dong, F., Birmili, W., and Wiedensohler, A.: First long-term study of particle number size distributions and new particle formation events of regional aerosol in the North China Plain, Atmos. Chem. Phys., 11, 1565–1580, doi:10.5194/acp-11-1565-2011, 2011.

Sipilä, M., Berndt, T., Petäjä, T., Brus, D., Vanhanen, J., Stratmann, F., Patokoski, J., Mauldin III, R. L., Hyvärinen, A.-P., Lihavainen, H., and Kulmala, M.: The Role of Sulfuric Acid in Atmospheric Nucleation, Science, 327, 1243–1246, doi:10.1126/science.1180315, 2010.

Sogacheva, L., Dal Maso, M., Kerminen, V.-M., and Kulmala, M.: Probability of nucleation events and aerosol particle concentration in different air mass types arriving at Hyytiala southern Finland, based on back trajectories analysis, Boreal Environ. Res., 10, 479–491, 2005.

Stanier, C. O., Khlystov, A. Y., and Pandis, S. N.: Ambient aerosol size distributions and number concentrations measured during the Pittsburgh Air Quality Study (PAQS), Atmos. Environ., 38, 3275–3284, doi:10.1016/j.atmosenv.2004.03.020, 2004.

Twomey, A.: Pollution and the planetary albedo, Atmos. Environ., 8, 1251–1256, doi:10.1016/0004-6981(74)90004-3, 1974.

Twomey, S., Piepgrass, M., and Wolfe, T. L.: An assessment of the impact of pollution on global cloud albedo, Tellus, 36B, 356–366, doi:10.1111/j.1600-0889.1984.tb00254.x, 1984.

Twomey, S.: Aerosols, clouds and radiation, Atmos. Environ., 25A, 2435–2442, doi:10.1016/0960-1686(91)90159-5, 1991.

ACPD
13, 22337–22381, 2013

Vehkamäki, H., Dal Maso, M., Hussein, T., Flanagan, R., Hyvärinen, A., Lauros, J., Merikanto, J., Mönkkönen, P., Pihlatie, M., Salminen, K., Sogacheva, L., Thum, T., Ruuskanen, T. M., Keronen, P., Aalto, P. P., Hari, P., Lehtinen, K. E. J., Rannik, Ü., and Kulmala, M.: Atmospheric particle formation events at Värriö measurement station in Finnish Lapland 1998–2002, Atmos. Chem. Phys., 4, 2015–2023, doi:10.5194/acp-4-2015-2004, 2004.

Wang, Z. B., Hu, M., Yue, D. L., Zheng, J., Zhang, R. Y., Wiedensohler, A., Wu, Z. J., Nieminen, T., and Boy, M.: Evaluation on the role of sulfuric acid in the mechanisms of new particle formation for Beijing case, Atmos. Chem. Phys., 11, 12663–12671, doi:10.5194/acp-11-12663-2011, 2011.

Wichmann, H. E. and Peters, A.: Epidemiological evidence of the effects of ultrafine particle exposure, Philos. T. R. Soc. Lond. Ser. A, 358, 2751–2769, doi:10.1098/rsta.2000.0682, 2000.

Woo, K. S., Chen, D. R., Pui, D. Y. H., and McMurry, P. H.: Measurements of Atlanta aerosol size distributions: observations of ultrafine particle events, Aerosol Sci. Tech., 34, 75–87, doi:10.1080/02786820120056, 2001.

Wu, Z. J., Hu, M., Liu, S., Wehner, B., Bauer, S., Maßling, A., Wiedensohler, A., Petäjä, T., Dal Maso, M., and Kulmala, M.: New particle formation in Beijing, China: Statistical analysis of a 1-year data set, J. Geophys. Res., 112, D09209, doi:10.1029/2006JD007406, 2007.

Xu, P. J., Wang, W. X., Yang, L. X., Zhang, Q. Z., Gao, R., Wang, X. F., Nie, W., and Gao, X. M.: Aerosol size distributions in urban Jinan: Seasonal characteristics and variations between weekdays and weekends in a heavily polluted atmosphere, Environ. Monit. Assess., 179, 443–456, doi:10.1007/s10661-010-1747-2, 2011.

Yao, X. H., Choi, M. Y., Lau, N. T., Lau, A. P. S., Chan, C. K., and Fang, M.: Growth and Shrinkage of New Particles in the Atmosphere in Hong Kong, Aerosol Sci. Tech., 44, 639–650, doi:10.1080/02786826.2010.482576, 2010.

Yue, D. L., Hu, M., Zhang, R. Y., Wang, Z. B., Zheng, J., Wu, Z. J., Wiedensohler, A., He, L. Y., Huang, X. F., and Zhu, T.: The roles of sulfuric acid in new particle formation and growth in the mega-city of Beijing, Atmos. Chem. Phys., 10, 4953–4960, doi:10.5194/acp-10-4953-2010, 2010.

Yue, D. L., Hua, M., Zhang, R. Y., Wu, Z. J., Su, H., Wang, Z. B., Peng, J. F., He, L. Y., Huang, X. F., Gong, Y. G., and Wiedensohler, A.: Potential contribution of new particle formation to cloud condensation nuclei in Beijing, Atmos. Environ., 45, 6070–6077, doi:10.1016/j.atmosenv.2011.07.037, 2011.

ACPD
13, 22337–22381, 2013

Zhang R. Y., Suh, I., Zhao, J., Zhang, D., Fortner, E. C., Tie, X. X., Molina, L. T., and Molina, M. J.: Atmospheric New Particle Formation Enhanced by Organic Acids, Science, 304, 1487–1489, doi:10.1126/science.1095139, 2004.

Zhang, Y. M., Zhang, X. Y., Sun, J. Y., Lin, W. L., Gong, S. L., Shen, X. J., and Yang, S.: Characterization of new particle and secondary aerosol formation during summertime in Beijing, China, Tellus, 63B, 382–394, doi:10.1111/j.1600-0889.2011.00533.x, 2011.

ACPD

13, 22337–22381, 2013

Table 1. Instruments used in this study.

Measurements	Instruments
Aerosol particles 6–800 nm	DMPS (University of Helsinki)
Air ions 0.8–42 nm	AIS (Airel Ltd., Estonia)
$PM_{2.5}$	TEI SHARP-5030
O_3	TEI 49i
SO_2	TEI 43i
Metrological parameters (Air temperature, global radiation, wind, relative humidity)	CAMPBELL CR3000-TD

ACPD
13, 22337–22381, 2013

Table 2. Aerosol population statistics.

	Mean	5-perc.	25-perc.	Median	75-perc.	95-perc.
Total N [cm^{-3}]	23 300	9300	14 600	20 000	26 400	38 700
Ion clusters [cm^{-3}]	840	240	600	770	970	1450
Nucl. mode [cm^{-3}]	6700	960	2100	3500	6000	14 300
Aitken mode [cm^{-3}]	9500	3700	6100	8500	11 500	18 700
Accu. mode [cm^{-3}]	7100	2500	4700	6600	9100	12 600
$PM_{2.5}$[$\mu g\, m^{-3}$]	90	24	47	79	116	194
CS [$10^{-2}\, s^{-1}$]	5.4	1.7	3.0	4.1	5.6	7.7

ACPD
13, 22337–22381, 2013

Table 3. Event statistics.

	Event days	Non-event days	Undefined/no data
November (18–30)	1	5	8
December	4	23	4
January	7	13	11
February	7	12	10
March	7	12	16
TOTAL	26	65	45

ACPD
13, 22337–22381, 2013

Table 4. Aerosol numbers (cm^{-3}) in Nanjing, Shanghai, and around the world.

	10–100 nm	100–500 nm	
Shanghai, CN	28 511	1676	Gao et al. (2009)
Nanjing, CN	13 000	6200	This work
Alkmaar, NL	18 300	2120	Ruuskanen et al. (2001)
Erfurt, DE	17 700	2270	Wichmann and Peters (2000)
Helsinki, FI	16 200	973	Ruuskanen et al. (2001)
Pittsburgh, US	14 300	2170	Stanier et al. (2004)
Atlanta, US	21 400	n/a	Woo et al. (2001)

ACPD
13, 22337–22381, 2013

Table 5. Event characteristics.

	Mean	5-perc.	25-perc.	Median	75-perc.	95-perc.
J_6[$cm^{-3}\,s^{-1}$] (observed)	1.1	0.25	0.5	0.8	1.2	3.5
J_2[$cm^{-3}\,s^{-1}$] (calculated)	33.2	2.6	14.8	23.9	56.8	75.6
GR 6–30 nm (DMPS) [nmh^{-1}]	8.5	4.5	6.1	6.9	10.9	15.4
GR 3–7 nm (AIS) [$nm\,h^{-1}$]	6.3	2.4	4.5	5.9	7.9	11.8
GR 7–30 nm (AIS) [$nm\,h^{-1}$]	8.0	3.5	5.2	6.7	8.2	16.0
CS [$10^{-2}\,s^{-1}$]	2.4	0.9	2.0	2.5	3.1	3.8
Q[$10^6\,cm^{-3}\,s^{-1}$]	3.8	1.0	2.2	3.0	5.5	7.5

GR = growth rate, Q = source of condensable vapors

ACPD
13, 22337–22381, 2013

Table 6. Ion and total nucleation rates at different diameters, mean values.

	AIS (ions)	DMPS	AIS/DMPS
J_2[cm^{-3} s^{-1}]	0.02	33.2*	0.002
J_6[cm^{-3} s^{-1}]	0.05	1.1	0.046

* calculated value

ACPD
13, 22337–22381, 2013

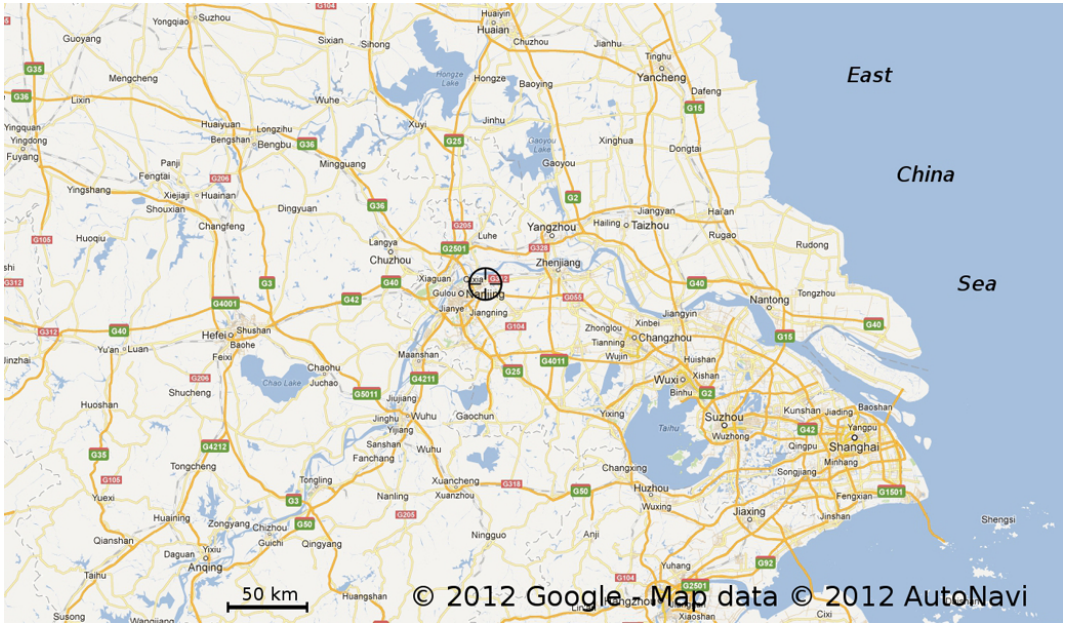

Fig. 1. Location of the SORPES measurement station within East China and the Yangtze River Delta (YRD).

ACPD
13, 22337–22381, 2013

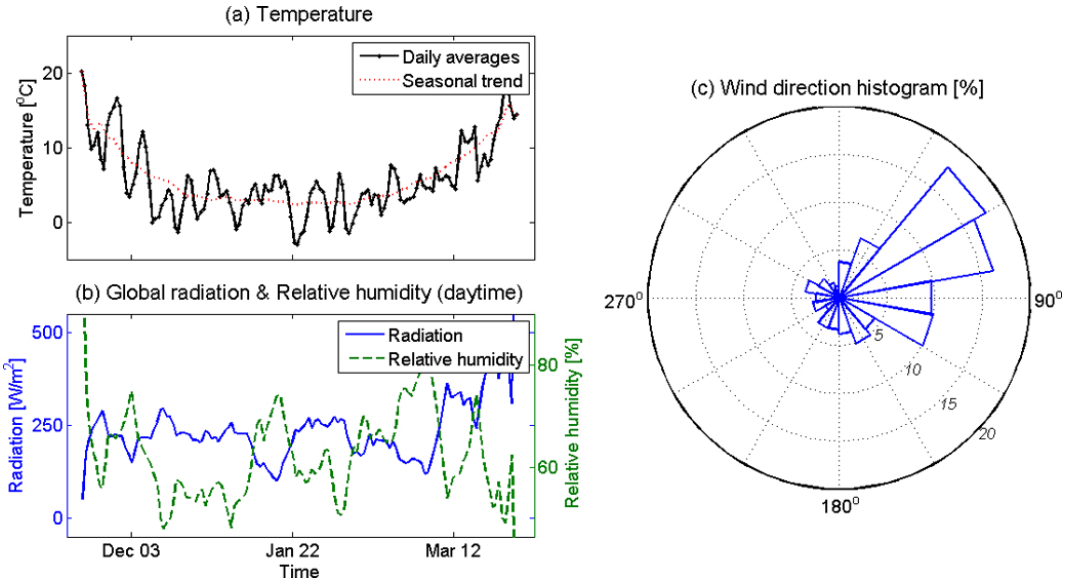

Fig. 2. Meteorological conditions during the measurement period 18 November–31 March. **(a)** Temperature with daily averages and seasonal trend. **(b)** Global radiation and relative humidity. **(c)** Wind direction.

ACPD
13, 22337–22381, 2013

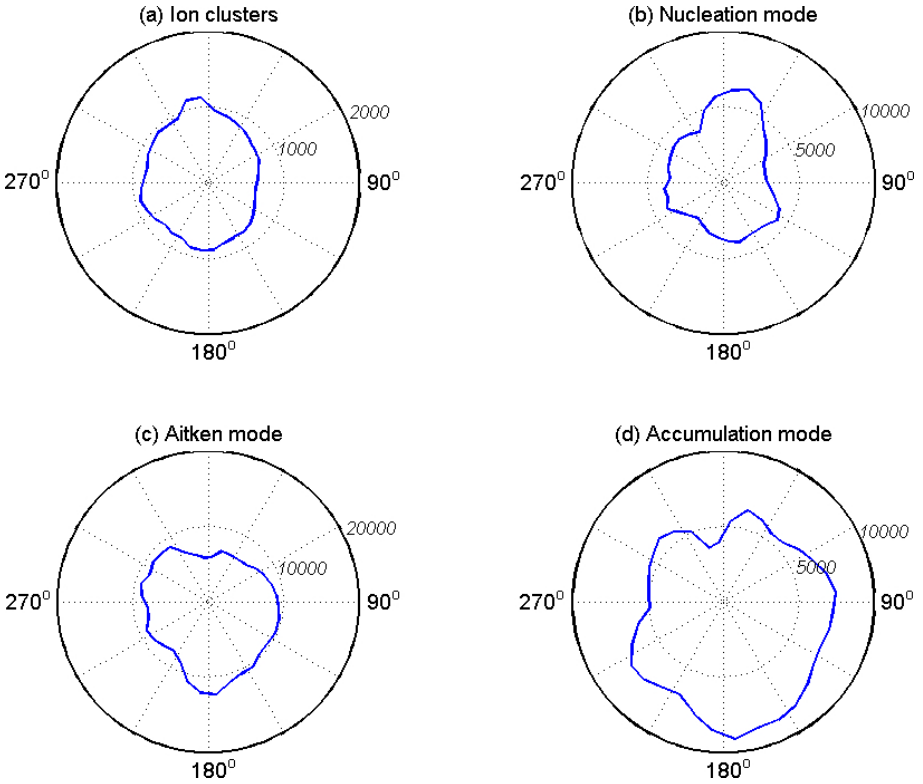

Fig. 3. Air ion and aerosol mode concentrations (all cm^{-3}) as a function of wind direction. **(a)** Ion clusters < 2 nm. **(b)** Nucleation mode 6–25 nm. **(c)** Aitken mode 25–90 nm. **(d)** Accumulation mode 90–800 nm.

ACPD
13, 22337–22381, 2013

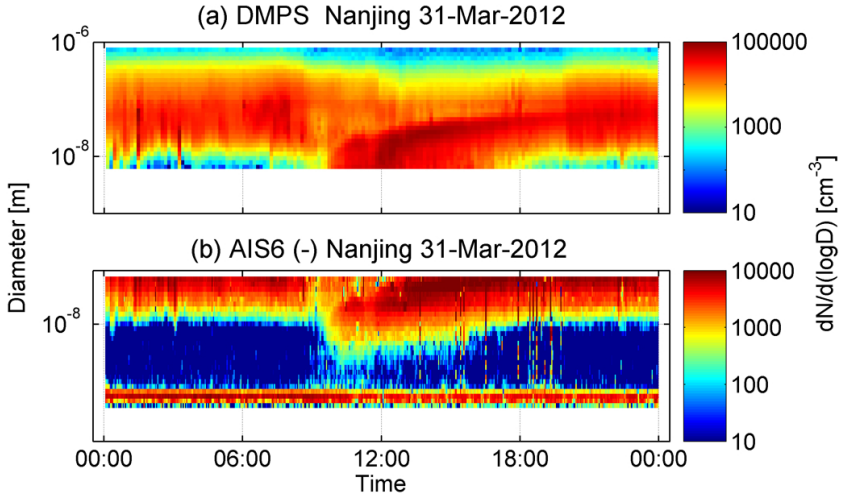

Fig. 4. Example of a typical particle formation event seen with both the AIS **(b)** and the DMPS **(a)**. Note the difference in color scale. Typical for particle formation events observed at the SORPES station is the gap visible in the AIS data, indicating that the neutral pathway dominates particle formation.

ACPD
13, 22337–22381, 2013


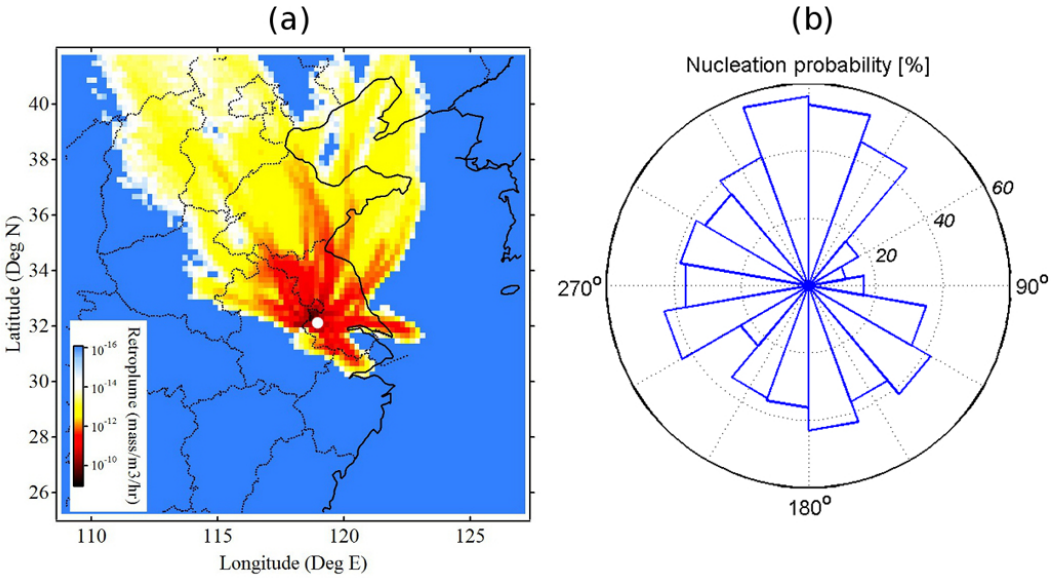

Fig. 5. (a) Retroplume for event days in a map of eastern China. The measurement site is marked by a dot. **(b)** Observed nucleation probability at the site as a function of the direction of the incoming air mass.

ACPD
13, 22337–22381, 2013

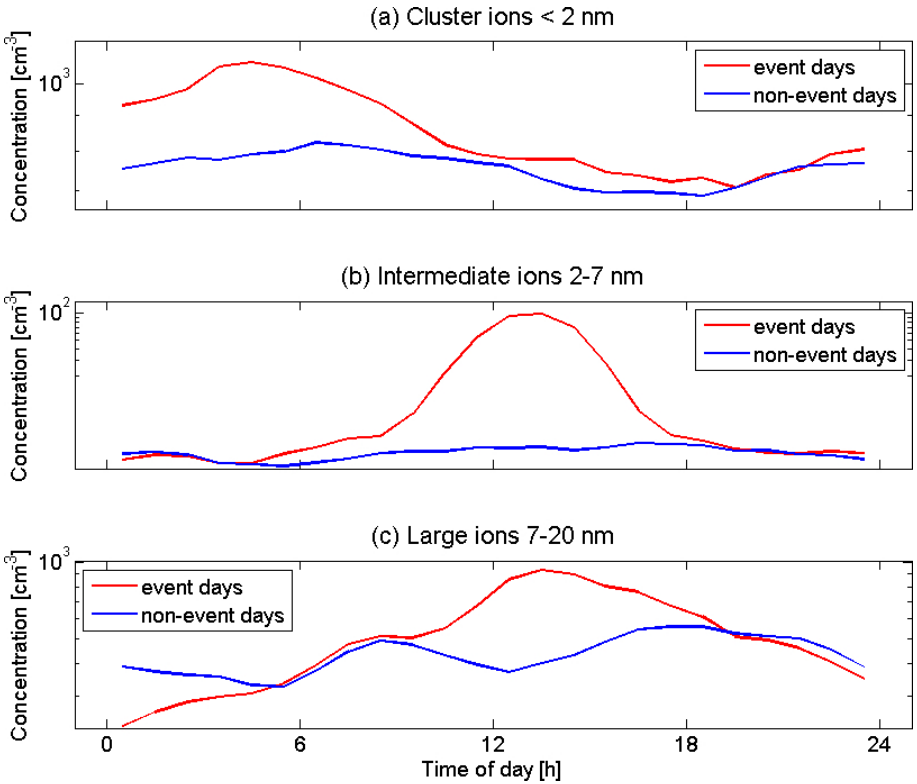

Fig. 6. Median diurnal cycles for different ion sizes, separated for days with and without new particle formation (event/non-event days). **(a)** Cluster ions < 2 nm. **(b)** Intermediate ions 2–7 nm. **(c)** Large ions 7–20 nm. Concentrations refer to the sum of positive and negative ions.

ACPD
13, 22337–22381, 2013

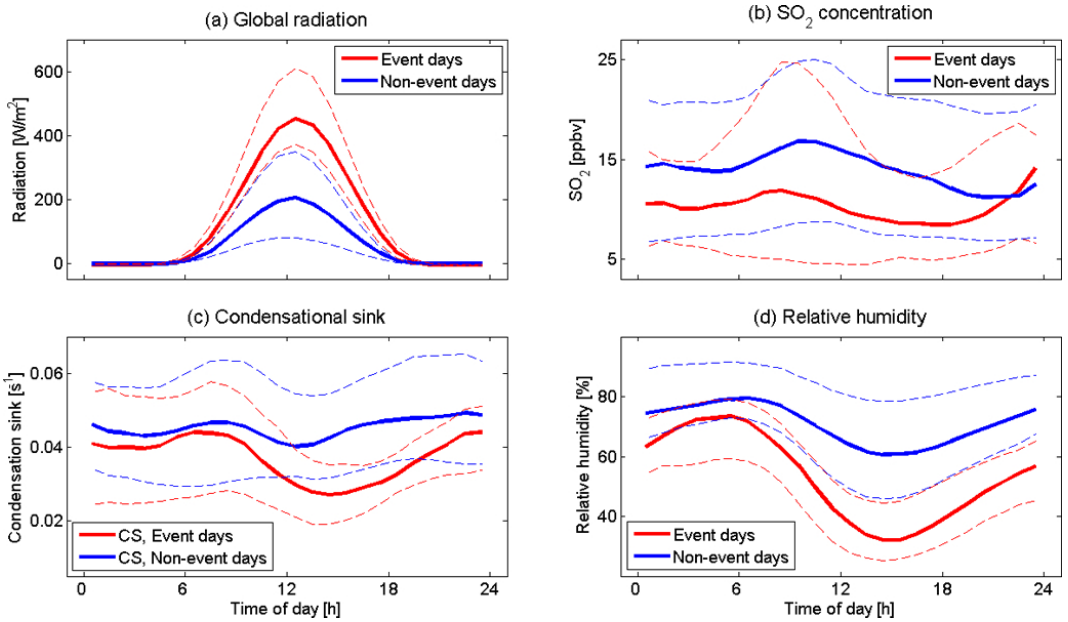

Fig. 7. Diurnal cycles of median values of relevant parameters for days with and without new particle formation. The dashed lines represent the respective quartiles. **(a)** Global radiation. **(b)** SO_2 concentration. **(c)** Condensational sink. **(d)** Relative humidity.

ACPD
13, 22337–22381, 2013

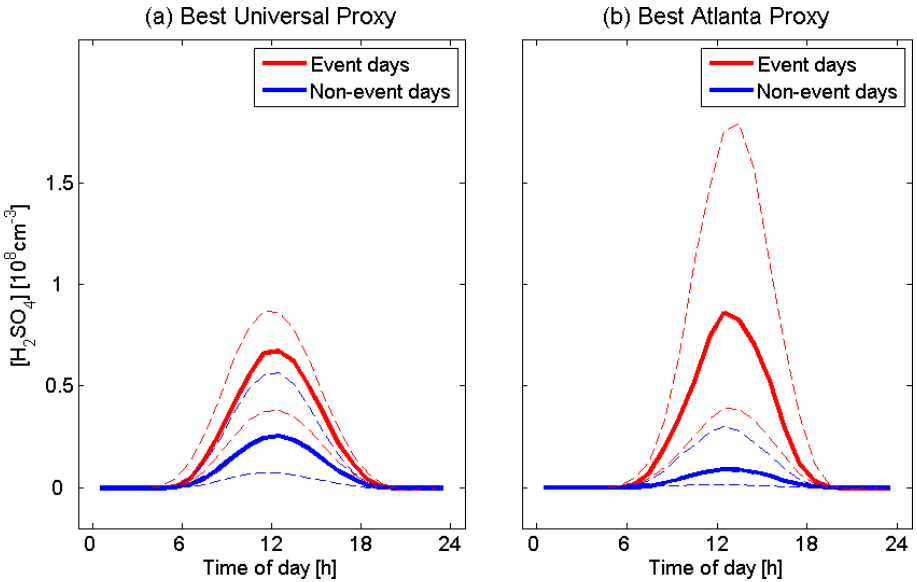

Fig. 8. Diurnal cycles of median values of two sulfuric acid proxies according to Mikkonen et al. (2011). Separated for days with and without new particle formation. The dashed lines represent the respective quartiles. **(a)** Best Universal proxy. **(b)** Best Atlanta proxy.

ACPD
13, 22337–22381, 2013

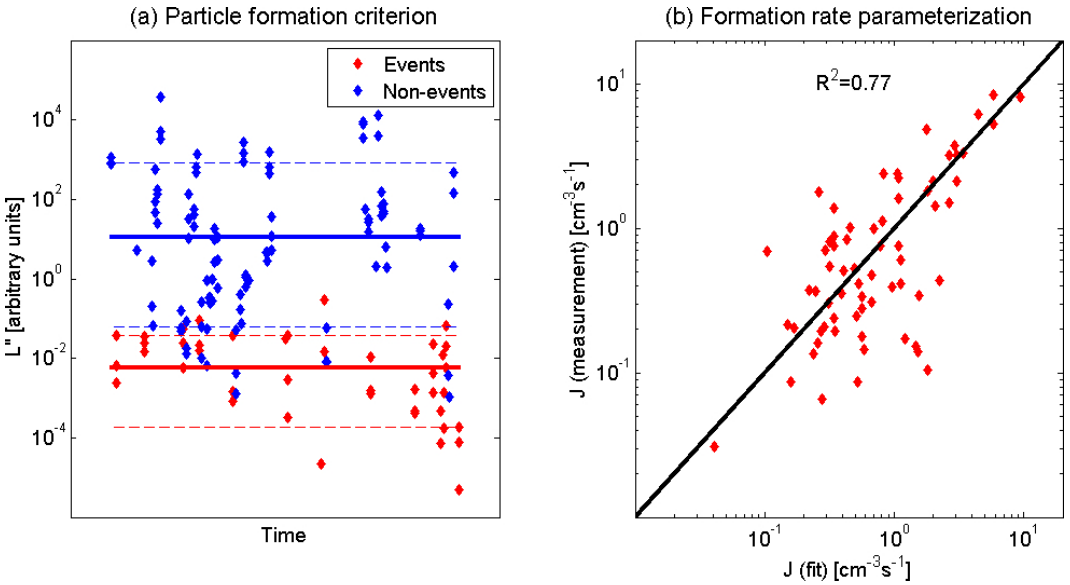

Fig. 9. Description of central particle formation characteristics as a function of observations of radiation, condensational sink, relative humidity, and SO_2 concentration. See respective sections for equations. **(a)** Particle formation criterion with quartiles. Note that the upper and lower quartile for events and non-events, respectively, do not overlap. **(b)** Particle formation rate J_6 parameterization with best fit. R^2 = 0.77.

ACPD
13, 22337–22381, 2013